# Topological Folding and Proteolysis Profile of P-glycoprotein in Membranes of Multidrug-Resistant Cells: Implications for the Drug-Transport Mechanism†

Mei Zhang,‡ Guichun Wang,‡ Adam Shapiro,§ and Jian-Ting Zhang*,‡

*Department of Physiology and Biophysics, University of Texas Medical Branch, Galveston, Texas 77555-0641, and British Columbia Cancer Center, 601 West 10th Avenue, Vancouver, Canada V5Z 1L3*

*Received February 20, 1996; Revised Manuscript Received May 7, 1996*⊗

ABSTRACT: P-glycoprotein (Pgp)[1] is a polytopic membrane protein and functions as an energy-dependent drug efflux pump. It is responsible for multidrug resistance (MDR) in cancer cell lines. Recently, the topological structure of Pgp has been investigated. However, the results are in dispute. A major question concerning the Pgp topology is the membrane orientation of the loop linking TM4 and TM5 (loop 4) and the loop linking TM8 and TM9 (loop 8). In this study, we generated polyclonal antibodies specific to these two loops. In combination with a panel of other well-characterized site-specific polyclonal and monoclonal antibodies of Pgp, we tested the membrane orientation of these two loops of Pgp in multidrug-resistant cells using immunocytochemistry and proteolysis/membrane protection assay. Our results showed that (1) both loops 4 and 8 are located extracellularly whereas other domains, such as the ATP-binding sites, are in the cytoplasm and (2) proteolysis of Pgp is not a random event and the trypsin-sensitive sites are cleaved in orders. Since the Pgp was not genetically manipulated in this study, in contrast to previous studies, we believe that naturally expressed Pgp molecules have an unconventional topology. We speculate that this alternate topology of Pgp may represent a different functional state of the protein. Further detailed analysis of Pgp topology will help to understand the fundamental mechanism of drug transport by Pgp.

P-glycoprotein (Pgp)[1] is a polytopic plasma membrane protein with a molecular weight of 130−180 kDa (Gottesman & Pastan, 1993; Borst et al., 1993; Childs & Ling, 1994). Overexpression of Pgp causes multidrug resistance (MDR) which may be responsible for the failure of cancer chemotherapy. Pgp belongs to a superfamily of ATP-binding cassette (ABC) transporter (Higgins, 1992) or traffic ATPases (Doige & Ames, 1993) and is thought to function as a drug efflux pump supported by energy from ATP hydrolysis. Pgp has a broad spectrum of drug substrates including vinca alkaloids, anthracyclines, epidophyllotoxins, and antimicrotubule drugs.

Pgp consists of two homologous halves with each containing six putative transmembrane (TM) segments linked by loops of various lengths and a hydrophilic ATP-binding domain (Gottesman & Pastan, 1993; Childs & Ling, 1994). Epitope mapping and immunocytochemistry studies using monoclonal antibodies MRK16 (Georges et al., 1993), C219 (Kartner et al., 1985), and MM4.17 (Cianfriglia et al., 1994) have confirmed the cytoplasmic location of the ATP-binding domains and the extracellular location of the loop linking the putative TM1 and TM2 and the loop linking the putative TM7 and TM8. The extracellular location of the loop linking the putative TM1 and TM2 is also supported by studies using cell-free and frog oocyte expression systems (Zhang & Ling, 1991; Zhang et al., 1993; Skach & Lingappa, 1993). However, topologies of Pgp different from prediction have been observed in cell-free (Zhang & Ling, 1991; Zhang et al., 1993; Skach et al., 1993), *Xenopus* oocyte (Skach et al., 1993), and bacteria (Bibi & Béjà, 1994; Béjà & Bibi, 1995) expression systems. The major difference between the conventional and unconventional models is the membrane sidedness of loop 4 (between TM4 and TM5) and loop 8 (between TM8 and TM9).

In this study, we generated and used a panel of site-specific polyclonal and monoclonal antibodies to approach the topology of Pgp naturally expressed in MDR cells in an attempt to determine the membrane orientation of loop 4 and loop 8. Our results indicate that both loops 4 and 8 are detected on the outside of cells and, therefore, the unconventional topology of Pgp exists in the MDR cells.

## MATERIALS AND METHODS

*Materials*. Plasmid pGEM-4z and restriction enzymes were obtained from Promega and New England Biolabs. pGEX-3X, pGEX-2T, and glutathione-conjugated Sepharose 4B were purchased from Pharmacia. The ImmunoPure Ag/Ab immobilization kit was obtained from Pierce. Avidin, biotin, biotinylated anti-mouse IgG, biotinylated anti-rabbit IgG, and ExtrAvidin peroxidase were purchased from Vector. Thrombin, trypsin, 3,3′-diaminobenzidine tetrahydrochloride (DAB), Freund's adjuvant, FITC-conjugated anti-mouse and anti-rabbit IgG, normal mouse IgG, normal goat serum, and other chemicals were from Sigma Chemical Co.

*Cell Lines*. CHO cell line Aux B1, colchicine-selected multidrug-resistant subclone $CH^RB30$, and the vinblastine-selected multidrug-resistant human ovarian cancer cell line SKOV/VLB were gifts from Dr. Victor Ling. The CHO cell

† This work was supported by National Institutes of Health Grant CA 64539 and by a grant from the U.S. Army Research and Development Command.

* Corresponding author. Tel 409-772-3434; Fax 409-772-3381.
‡ University of Texas Medical Branch.
§ B.C. Cancer Center.

⊗ Abstract published in *Advance ACS Abstracts,* July 15, 1996.

[1] Abbreviations: Pgp, P-glycoprotein; MDR, multidrug resistance; ABC, ATP-binding cassette; mAb, monoclonal antibody; pAb, polyclonal antibody; TM, transmembrane; GST, glutathione *S*-transferase; A/M, acetone/methanol; PF, paraformaldehyde; Ag, antigen.

S0006-2960(96)00400-X CCC: $12.00 © 1996 American Chemical Society

lines were maintained in α-MEM medium containing 10% FCS. Colchicine was added to the media for the maintenance of drug-resistant $CH^RB30$ cells at a final concentration of 30 μg/mL. The SKOV/VLB cell line was maintained in α-MEM medium containing 15% FCS and 1 μg/mL vinblastine.

*Antibodies*. Monoclonal antibodies C219 and C494 were gifts from Dr. Victor Ling. The epitopes of these two antibodies have been mapped (Georges et al., 1990; also see Figure 1). Polyclonal antibody 5 from Dr. Susan B. Horwitz was generated against a synthetic peptide of loop 8 of mouse Pgp (Greenberger et al., 1991). Only 2 of the 19 amino acids in the synthetic peptides are different between mouse and human Pgp and apparently the pAb 5 reacts also with human Pgp. The mAb MM4.17 was a gift from Dr. Maurizio Cianfriglia, and its epitope has been mapped to loop 7 of Pgp (Cianfriglia et al., 1994). Monoclonal antibodies MD-1 and MD-7 were generated against purified hamster Pgp, and their epitopes have been mapped to 22 and 11 amino acid residues in the linker region and loop 8, respectively (Shapiro et al., 1996). These two mAbs have been shown to react with human Pgp.

*Construction of Fusion Protein Expression Plasmids*. A 200 bp *Nde*I−*Nde*I cDNA fragment was released from a full-length Chinese hamster *pgp1* cDNA (Endicott et al., 1991). It was separated and purified by electrophoresis on a 2% agarose gel and was then subcloned into the *Hin*cII site of pGEM-4z. By a sequential treatment of this recombinant DNA with *Nco*I, Klenow polymerase, and *Bam*HI, a cDNA fragment encoding loop 4 (the loop linking putative TM4 and TM5, amino acids 241−289) of Pgp was isolated and ligated between the *Bam*HI and *Sma*I sites of the pGEX-2T vector containing the GST (glutathione *S*-transferase) gene. The resultant plasmid was named pGST-PgpL4.

A cDNA fragment encoding loop 8 (the loop linking putative TM8 and TM9) of Pgp was made by the polymerase chain reaction (PCR) using oligonucleotides 5′-TGGAGAGATCCTCAC-3′ (from the Pgp sequence) and 5′-TAATACGACTCACTATAGGG-3′ (T7 promoter sequence) as sense and antisense primers, respectively, and Chinese hamster *pgp1* cDNA as template. The PCR product was treated with T4 DNA polymerase to blunt each end and purified before ligation into the *Hin*cII site of pGEM-4z. By digestion of this recombinant DNA with *Hin*dIII and *Hin*cII, a 200 bp cDNA fragment was isolated and treated with *Tru*9I and Klenow polymerase. The final *Hin*dIII-*Tru*9I cDNA fragment encoding amino acids 778−822 of Pgp was subcloned into the *Sma*I site of pGEX-3X to generate the plasmid pGST-PgpL8. Both pGST-PgpL4 and pGST-PgpL8 were sequenced to confirm the correct reading frame and to eliminate any potential mutations introduced by PCR.

*Generation and Purification of Fusion Proteins*. Two hundred milliliters of overnight cultures of *Escherichia coli* transformed with pGEX (−2T or −3X), pGST-PgpL4, or pGST-PgpL8 plasmids was added to 2 L of YT medium containing 2% glucose and 100 μg/mL ampicillin and grown at 37 °C to an $OD_{600}$ of 1−2. IPTG was then added to a final concentration of 0.1 mM, and the cells were allowed to grow for an additional 3 h at 37 °C before harvest by centrifugation (5600*g*) for 10 min at 4 °C. The cell pellet was resuspended in 100 mL of ice-cold PBS, and cells were then disrupted by sonication. Triton X-100 was added to cells harboring pGEX or pGST-PgpL4 plasmid to a final concentration of 1%, and the cell lysate was centrifuged (12000*g*) for 10 min at 4 °C. The supernatant was mixed with 2 mL of 50% glutathione-conjugated Sepharose 4B and incubated for 30 min at room temperature with shaking. The GST from the pGEX plasmid and the GST-L4 fusion protein from the pGST-PgpL4 were isolated by centrifugation at 500*g* for 30 s. The Sepharose pellet was washed 3 times with 15 mL of PBS each time before resuspension in 2 mL of PBS. To isolate the Pgp portion (Pgp-L4) from the GST-L4 fusion protein, the glutathione-conjugated Sepharose-absorbed fusion proteins were digested with 50 units of thrombin for 4 h while being shaken at room temperature. The Sepharose beads containing GST and the supernatant containing the released Pgp-L4 peptide were separated by centrifugation at 500*g* for 30 s. Because of formation of inclusion bodies in cells harboring pGST-PgpL8 plasmid, the disrupted cells after sonication were dissolved in sample buffer and subjected to a 12.5% SDS−PAGE. Fusion protein GST-L8 was visualized by Coomassie blue staining, excised, and purified by electroelution (Harlow & Lane, 1988).

*Generation and Purification of Antibodies*. Approximately 500 μg each of the purified Pgp-L4 peptide and GST-L8 fusion protein in complete Freund's adjuvant was injected subcutaneously into New Zealand white rabbits. One hundred fifty micrograms of purified proteins in incomplete Freund's adjuvant was injected as first boost 30 days after the initial injection, and sera were collected 2−4 times in 1 month 7 days after each boost. These antisera were named αPgp-L4 and αPgp-L8, respectively. Preimmune sera were collected as control before all above steps were taken.

Affinity purification of the antisera was performed using an ImmunoPure Ag/Ab immobilization kit from Pierce following the supplier's instructions. Briefly, 2 mg of Pgp-L4 peptide or GST-L8 fusion protein was added to an Ag immobilization column and conjugated to an activated affinity chromatography gel after incubation at room temperature for 8 h. The column was then washed excessively with PBS before 1 mL of relevant crude antiserum was applied to the column and maintained at room temperature for 1 h. The affinity-bound antibodies were eluted with 0.1 M glycine (pH 2.8), immediately neutralized with 1 M Tris-HCl (pH 9.5), and concentrated by using a Centricon filtration unit (Amicon).

*Confocal Fluorescence Microscopy*. Parental Aux B1 and MDR $CH^RB30$ cells grown on a cover glass for 2 days were washed in TBS (10 mM Tris-HCl, pH 7.4, 0.9% NaCl) and fixed/permeabilized in acetone/methanol (50:50) for 5 min at room temperature. Following three washes with TBS, the cells were blocked by 10% skim milk in TBS for 2 h and then incubated with mAb C219 (1 μg/mL), affinity-purified αPgp-L4 (1:2000 dilution) or affinity-purified αPgp-L8 (1:1000 dilution) in TBS containing 1% skim milk for 2 h at room temperature. After three washes with TBS, the cells were incubated with either FITC-conjugated anti-mouse IgG (for mAb C219) or anti-rabbit IgG (for αPgp-L4 or αPgp-L8) for 30 min at room temperature. The fluorescence was detected with an Odyssey digital video confocal laser imaging system (Noram Instruments) coupled to a Nikon inverted microscope. Fluorescence was detected at 515 nm using an excitation of 488 nm.

*Immunocytochemical Staining*. $CH^RB30$ cells were grown overnight or for 2 days on a cover glass and were then fixed

and permeabilized with acetone/methanol (50:50) at 4 °C for 10 min or only fixed with 4% paraformaldehyde. After several washes with PBS, endogenous peroxidase and biotin-like activities were blocked by pretreatment with $H_2O_2$ and avidin/biotin, respectively. The fixed cells were then labeled with primary antibodies C219, affinity-purified αPgp-L4, or affinity-purified αPgp-L8, followed by biotinylated anti-mouse IgG or anti-rabbit IgG. The final staining with ExtrAvidin peroxidase and DAB was performed as described by Georges et al. (1990). For competition studies, the primary antibodies were incubated for 2 h with an excess amount of the C219 epitope peptide, purified Pgp-L4 peptide, or GST-PgpL4 fusion protein before being used for labeling cells. The labeled cells were counterstained with hematoxylin and mounted with Permount for visualization.

*Proteolysis/Membrane Protection Assay*. Membranes were isolated from $CH^RB30$, SKOV/VLB, and BC19/3 cells according to the method described previously by Riordan and Ling (1979). Sealed inside-out vesicles were prepared according to the procedure by Steck and Kant (1974). Briefly, 1 mg of crude membranes was diluted into 10 mL of 0.5 mM sodium phosphate buffer, pH 8.2 (PB). After 3 h of incubation on ice, the membranes were pelleted at 28000*g* for 30 min. The membrane pellet was then resuspended in 1 mL of PB buffer by using a 25 gauge needle and a 1 mL syringe. The membrane orientation was determined as described previously (Bender et al., 1971). Using this procedure, the sealed membrane vesicles isolated from both SKOV/VLB and BC19/3 cells are all inside out.

Trypsin digestion of 10 μg of inside-out membrane vesicles was performed at different conditions. After incubation of membrane with 0.2 μg (for 15 min), 0.2 μg (for 30 min), 3 μg (for 2 h), or 6 μg (for 2 h) of trypsin at 37 °C, the reaction was stopped by addition of PMSF to a final concentration of 10 mM and the membrane fraction was separated from trypsin by microcentrifugation at 4 °C. The final membrane pellet was immediately solubilized in SDS−PAGE sample buffer and used for electrophoresis.

*Characterization of the Orientation of Membrane Vesicles*. The membrane vesicle orientation was determined using marker enzyme acetylcholinesterase and $Na^+/K^+$-ATPase as described previously (Bender et al., 1971; Chifflet et al., 1988; Doige et al., 1992). Briefly, acetylcholinesterase activity was determined by incubating the sealed membrane vesicles (50 μg of protein) in the absence or presence of 0.1% Triton X-100 with 0.78 μM acetylthiocholine chloride and 0.625 mM DTNB [5,5′-dithiobis(2-nitrobenzoic acid)] in TBS containing 0.25 M sucrose. The reaction was performed at 37 °C for 20 min and stopped by addition of 10% SDS. Absorption at 412 nm wavelength was measured on a Shimatzu UV-160 spectrophotometer. The activity was calculated using purified acetylcholinesterase (Sigma) as standard. The $Na^+/K^+$-ATPase activity was determined by incubating 12 μg of membrane proteins in the absence or presence of 1 mM ouabain in the assay buffer (10 mM Tris-HCl, pH 7.4, 100 mM NaCl, 10 mM KCl, 3 mM $MgCl_2$, 0.02% $NaN_3$, 2 mM ATP). After 20 min of incubation at 37 °C, the reaction was stopped by addition of an equal volume of 6% SDS/3% ascorbate/0.5% ammonium molybdate in 0.5 M HCl. Products were stabilized by addition of the same volume of 2% sodium citrate/2% sodium arsenite/2% acetic acid. The absorption at 850 nm was measured on a Shimatzu UV-160 spectrophotometer. The activity was calculated according to Chifflet et al. (1988). The ouabain-sensitive ATPase activity reflects the $Na^+/K^+$-ATPase activity.

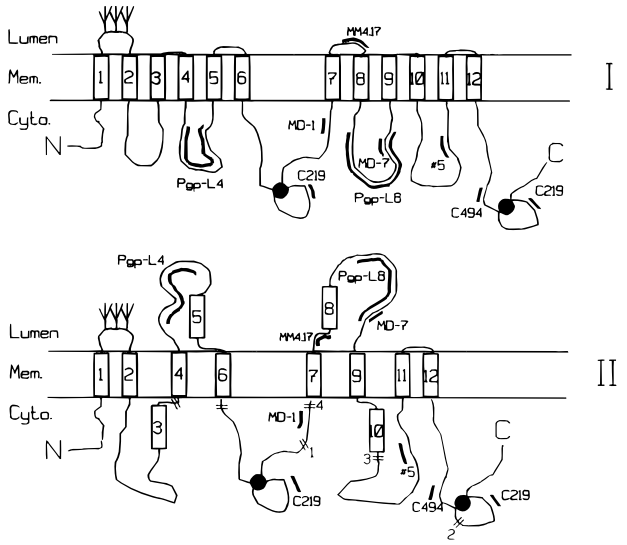


FIGURE 1: Topology of P-glycoprotein and positions of antibody epitopes. The model I structure is predicted on the basis of the hydropathy plot analysis of the amino acid sequence. The model II structure is one example of the alternate topologies observed with Pgp expressed in a heterologous expression system. The branched symbols indicate oligosaccharide chains. The solid circle represents the ATP-binding domain. The thick lines denote the relative positions of antibody epitopes. The symbol (═) indicates the trypsin cleavage sites deduced from Figure 5.

*Western Blot Analysis*. Purified fusion proteins or Pgp-L4 peptides and crude membranes isolated from MDR cells were subjected to SDS−PAGE. The fractionated proteins were then transferred to a PVDF membrane and probed with primary antibodies (mAb C219, C494, MD-1, and MD-7 at 1 μg/mL, MM4.17 at 2 μg/mL, pAb αPgp-L4 at 1:2000 dilution, αPgp-L8 at 1:1000 dilution, and antibody 5 at 1:1000) followed by a secondary antibody (peroxidase-conjugated anti-mouse IgG or anti-rabbit IgG at 1:2500 dilution) and detected by enhanced chemiluminescence using an ECL detection kit (Amersham). To strip the blot for reprobing, the blot was incubated at 50 °C in stripping buffer (62.5 mM Tris-HCl, pH 6.7, 100 mM β-mercaptoethanol, 2% SDS) for 25 min and washed in TBS 2 × 10 min at room temperature. The blot was then used for reprobing.

## RESULTS

*Both Polyclonal Antibodies αPgp-L4 and αPgp-L8 React with Pgp on Western Blot*. In the unconventional topology of Pgp, the loop linking TM4 and TM5 (loop 4) and the loop linking TM8 and TM9 (loop 8) are extracellular (model II, Figure 1). However, these two loops are intracellular in the conventional or predicted topology (model I, Figure 1). To determine the membrane orientation of these two loops in MDR cells, we generated site-specific polyclonal antibodies to these loops using fusion proteins as immunogens (see Materials and Methods). These two pAbs were named αPgp-L4 and αPgp-L8. Using Western blot analysis, both antibodies specifically reacted with their immunogen and no cross-reaction was detected (data not shown). To determine the specificity of αPgp-L4 and αPgp-L8 to Pgp, crude membranes were isolated from parental Aux B1 and multidrug-resistant $CH^RB30$ cells, and Pgp was separated on an SDS−PAGE. Figure 2 shows a Western blot of crude

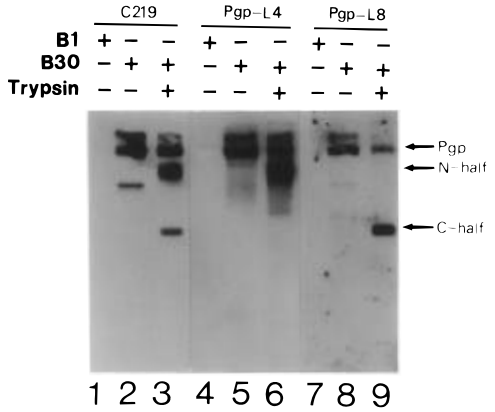


FIGURE 2: Characterization of the specificity of αPGp-L4 and αPgp-L8 antibodies to P-glycoprotein on $CH^RB30$ cells. Crude membranes were isolated from parental Aux B1 (lanes 1, 4, and 7) and multidrug resistant $CH^RB30$ cells (lanes 2, 5, and 8) and were used for Western blot analysis (10 $\mu$g of proteins in each lane). Monoclonal antibody C219 as well as the polyclonal antibodies αPgp-L4 and αPgp-L8 specifically detected the 180 kDa Pgp and its aggregated and degraded products (lanes 2, 5, and 8). No protein from Aux B1 cells was detected by any of these antibodies. After limited trypsin digestion (10 $\mu$g of protein was digested using 0.2 $\mu$g of trypsin for 30 min at 37 °C), Pgp from $CH^R30$ cells was cleaved into N- and C-terminal half fragments as detected by C219 (lane 3). As expected, only the N-half fragment was recognized by αPgp-L4 (lane 6) whereas the C-half was recognized by αPgp-L8 (lane 9). Lanes 3, 6, and 9 contains 6 $\mu$g of proteins.

membranes detected by monoclonal antibody (mAb) C219 as well as pAb αPgp-L4 and αPgp-L8. The mAb C219 (lane 2, Figure 2), pAb αPgp-L4 (lane 5, Figure 2), and pAb αPgp-L8 (lane 8, Figure 2) specifically detected a 180 kDa protein. This protein was not detected in the sensitive Aux B1 cells (lanes 1, 4, and 7, Figure 2). Endoglycosidase treatment reduced the size of the protein detected by these antibodies (data not shown), indicating that it is a glycoprotein. Additional bands of higher and lower molecular weight detected by these antibodies represent the aggregated and degraded products of Pgp.

*αPgp-L4 and αPgp-L8 React with N- and C-Terminal Half Molecules of Pgp, Respectively*. Previously, it has been shown that Pgp isolated from multidrug-resistant $CH^RB30$ cells can be cleaved into two halves with limited proteolysis using trypsin, and both halves react with the mAb C219 (Georges et al., 1991). To determine whether pAb αPgp-L4 and αPgp-L8 specifically react with N- and C-terminal halves of Pgp, respectively, we performed a limited trypsin digestion to cleave Pgp into two separate halves. As shown in Figure 2, both halves of Pgp react with the mAb C219 (lane 3, Figure 2). However, as expected, the pAb αPgp-L4 reacted only with the N-terminal half (lane 6, Figure 2), while the pAb αPgp-L8 reacted only with the C-terminal half (lane 9, Figure 2) of Pgp. Therefore, we conclude that we have generated site-specific pAb to putative loops 4 and 8 of Pgp.

*Both αPgp-L4 and αPgp-L8 React Predominantly with the Plasma Membranes of $CH^RB30$ Cells*. To confirm whether pAb αPgp-L4 and αPgp-L8 specifically detect Pgp on plasma membranes, we labeled fixed and permeabilized $CH^RB30$ cells with mAb C219, pAb αPgp-L4, and αPgp-L8. The binding was detected with FITC-conjugated secondary antibodies using confocal fluorescence microscopy (see Materials and Methods). As shown in Figure 3, mAb C219 (panel A), as well as pAb αPgp-L4 (panel C) and

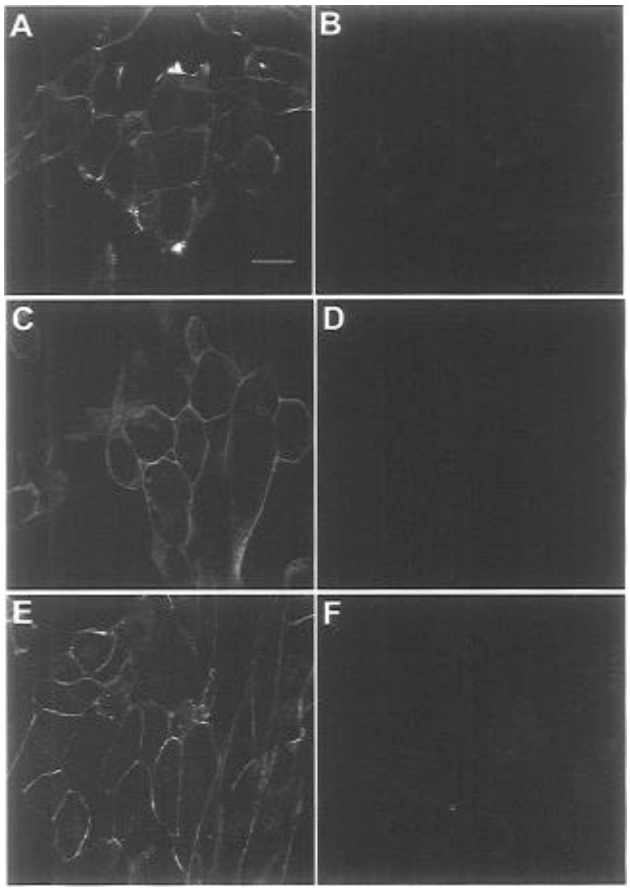


FIGURE 3: Immunofluorescence labeling of $CH^RB30$ cells using αPgp-L4 and αPgp-L8. Multidrug-resistant $CH^RB30$ cells were fixed and permeabilized with acetone/methanol and labeled with mAb C219 (panel A), pAb αPgp-L4 (panel C), or pAb αPgp-L8 (panel E). The labeling was detected using FITC-conjugated secondary antibodies and observed by confocal fluorescence microscopy. In the controls, cells were labeled using normal mouse IgG (panel B) and preimmune sera of αPgp-L4 (panel D) and αPgp-L8 (panel F). All three antibodies labeled predominantly on the plasma membranes. The bar in panel A denotes 10 $\mu$m. All photographs were taken with the same magnification.

αPgp-L8 (panel E) stained predominantly the plasma membrane of $CH^RB30$ cells. No signal was detected on plasma membranes in control experiments with either normal mouse IgG (panel B) or preimmune sera of αPgp-L4 (panel D) or αPgp-L8 (panel F). Under the same condition, no staining was observed with the parental Aux B1 cells (data not shown), consistent with the results on Western blot shown in Figure 2. These results indicate that the pAb αPgp-L4 and αPgp-L8 specifically react with Pgp both on Western blot and in plasma membranes of whole cells.

*Immunocytochemical Staining*. To investigate the membrane sidedness of loops 4 and 8 of Pgp in plasma membranes, we performed indirect whole-cell staining with the pAb αPgp-L4, αPgp-L8, and mAb C219 in permeabilized and nonpermeabilized conditions (see Materials and Methods). $CH^RB30$ cells were first fixed and permeabilized with acetone/methanol (A/M) or only fixed with paraformaldehyde (PF) and then probed with C219, αPgp-L4, or αPgp-L8. The secondary antibodies were biotinylated goat anti-mouse or goat anti-rabbit IgG. The staining was performed using ExtrAvidin peroxidase and DAB. As shown in Figure 4, specific staining of fixed and permeabilized (A/M) $CH^RB30$ cells was observed with mAb C219 (panel D), as well as

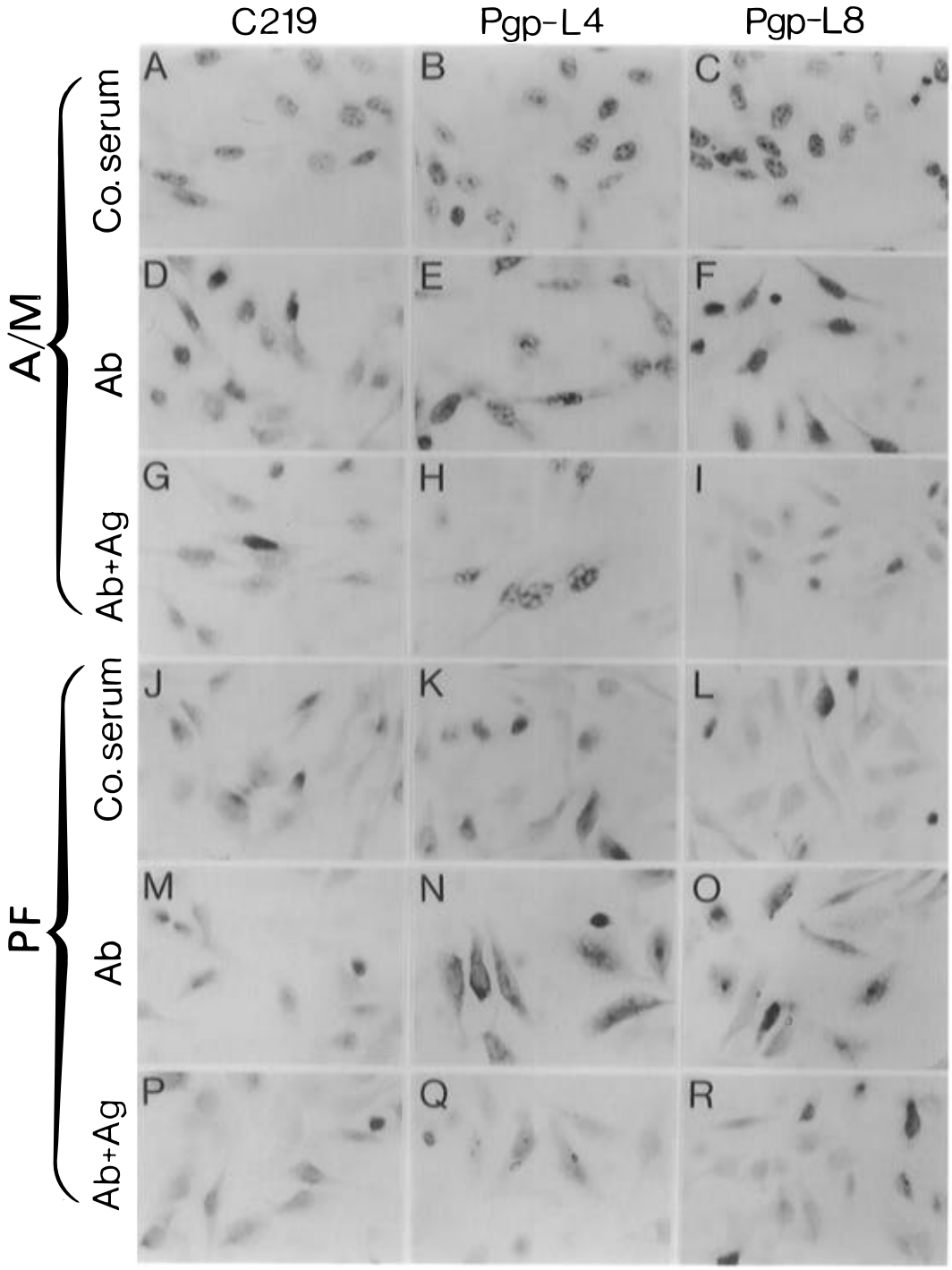


FIGURE 4: Immunocytochemistry staining of multidrug-resistant CH$^R$B30 cells with αPgp-L4 and αPgp-L8. CH$^R$B30 cells were grown on a cover glass and fixed and permeabilized with acetone/methanol (panels A−I) or only fixed with paraformaldehyde (panels J−R). The fixed cells were probed with either C219 (panels D, G, M, P), αPgp-L4 (panels E, H, N, Q), or αPgp-L8 (panels F, I, O, R). Normal mouse IgG (panels A and J), preimmune sera of αPgp-L4 (panels B and K), and αPgp-L8 (panels C and I) were used as controls at the same concentration as the antibodies. C219-epitope peptide analog (panels G and P), purified Pgp-L4 peptide (panels H and Q), or GST-L8 fusion proteins (panels I and R) were used to compete the Pgp-specific bindings of mAb C219, pAb αPgp-L4, and pAb αPgp-L8, respectively. Nuclei were stained using hematoxylin. A/M = acetone/methanol fixed; PF = paraformaldehyde fixed; Ab = antibodies; Ab + Ag = antibody preincubated with antigen; Co. serum = control IgG or preimmune serum.

pAb αPgp-L4 (panel E) and αPgp-L8 (panel F). The pAb αPgp-L4 and αPgp-L8 were also able to stain the nonpermeabilized (PF) cells (panels N and O). Monoclonal antibody C219, on the other hand, did not stain the nonpermeabilized cells (panel M), consistent with the intracellular location of the C219 epitope. This is further supported by the observation that mAb C219 stained the paraformaldehyde-fixed cells after permeabilization with Triton X-100 (data not shown). Normal mouse IgG (panels A and J), preimmune sera of pAb αPgp-L4 (panels B and K), and pAb αPgp-L8 (panels C and L) did not stain the cells fixed with acetone/methanol (panels A−C) or with paraformaldehyde (panels J−L). It should be noted that the staining of intact cells with pAb αPgp-L8 (panel O) was lower than that of the permeabilized cells. This suggests that loop 8 may be partially buried in the plasma membrane or it may exist in both extracellular and cytoplasmic locations (see Discussion).

Table 1: Activity of Marker Enzymes in Membrane Vesicles of SKOV/VLB Cells

| | enzyme activity (nmol mg$^{-1}$ min$^{-1}$) | |
|---|---|---|
| detergent[a] | − | + |
| acetylcholinesterase | 0.00 (3) | 2.07 ± 0.29 (3) |
| $Na^+/K^+$-ATPase | 10.4 ± 0.88 (3) | 11 ± 2.5 (3) |

[a] 0.1% Triton X-100 was used for the assay of total acetylcholinesterase activity (extracellular marker), and 0.8 mM CHAPS was used for the assay of total $Na^+/K^+$-ATPase activity (cytoplasmic marker). Activity measured in the presence of detergent represents the total activity derived from both inside-out and outside-out vesicles. Acetylcholinesterase was detected only when the vesicles were permeabilized whereas the $Na^+/K^+$-ATPase activity was detected in the intact vesicles. $n = 3$.

To determine the cell-labeling specificity to Pgp with mAb C219, pAb αPgp-L4, and αPgp-L8, we stained cells with these antibodies in the presence of excess amounts of the C219 epitope peptide (panels G and P), purified PgpL4 peptide (panels H and Q), and GST-PgpL8 fusion proteins (panels I and R), respectively (Ab + Ag). As shown in Figure 4, the preincubation prevented the staining of $CH^R$-B30 cells, suggesting that the staining is specific for Pgp. However, the nonrelevant peptide antigens did not block the antibody binding (data not shown). Together, the above immunocytochemical results suggest that the epitopes for mAb C219 are located inside cells whereas the epitopes for pAb αPgp-L4 and αPgp-L8 can be detected extracellularly.

*Loop 8 of Pgp in Inside-Out Membrane Vesicles Is Resistant to Trypsin Digestion.* To confirm that loops 4 and 8 of Pgp in MDR cells were located extracellularly, we performed proteolysis/membrane protection assay and Western blot of isolated membrane vesicles. We used the human multidrug-resistant SKOV/VLB cells (Bradley et al., 1989), from which all vesicles isolated are inside out (Table 1) as determined using acetylcholinesterase (extracellular marker). This is confirmed by another marker $Na^+/K^+$-ATPase (cytoplasmic side marker) (Table 1). Meanwhile, we obtained a mAb MD-7 which has an epitope in loop 8 (Shapiro et al., 1996). Furthermore, an advantage for using human MDR cells is that more site-specific antibodies are available and they can be used as controls in the proteolysis study (see Figure 1 for locations in Pgp of each antibody epitope used in this study).

Figure 5A shows the trypsin digestion profile of Pgp detected by the mAb MD-7. Under mild conditions, peptides indicated as C (C-half) were detected (lanes 2 and 3, Figure 5A). More extensive trypsin digestion generated smaller fragments labeled as X, Y, and Z, respectively (lanes 4 and 5, Figure 5A). All these fragments were presumably derived from the C-half molecule with the epitope for the mAb MD-7. The smallest trypsin-resistant fragment detected by the mAb MD-7 has an apparent molecular mass of 17 kDa (peptide Z). It is possible that the generation of these fragments represents the progressive digestion of the C-terminal half molecule of Pgp and peptide Z represents the minimum membrane-protected fragment containing loop 8 with the mAb MD-7 epitope.

To determine the likelihood of the above possibility, we stripped the same blot and probed it with other mAbs or site-specific pAbs. Figure 5B shows the same blot from Figure 5A probed with the mAb C219. Only two peptide fragments indicated as N and C were detected by C219 (lanes 2−5, Figure 5B). Peptide N did not react with the mAb MD-7 and represents the N-terminal half molecule (lanes 2−5, Figure 5A; see also Figure 2). The mAb C494, on the other hand, detected peptide C (lanes 2−5, Figure 5C). Together, these results suggest that peptides N and C represent the N- and C-terminal half molecules, respectively. These results are consistent with the previous studies which showed that the mAb C219 has two epitopes, one in each ATP-binding domain, and the mAb C494 has only one epitope in the C-terminal half molecule (Georges et al., 1990) and Pgp can be cleaved into two halves by trypsin (Georges et al., 1991; see Figure 1 for cleavage site 1).

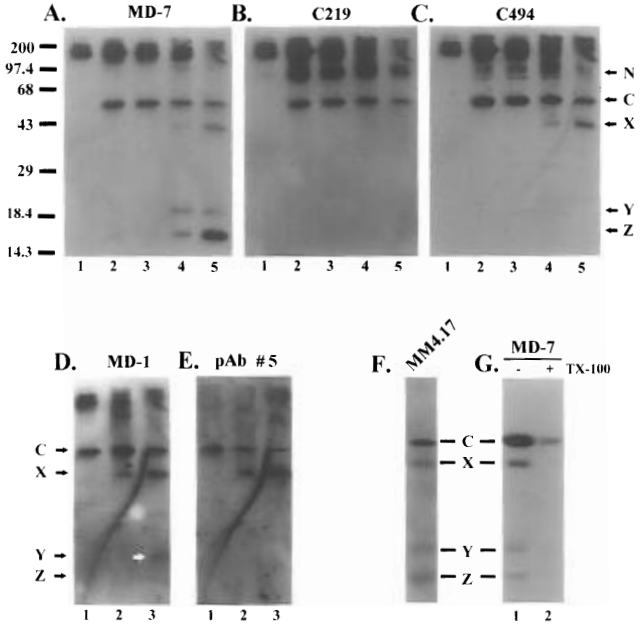


FIGURE 5: Proteolysis profile of P-glycoprotein. (A−C) Trypsin cleavage profile of human P-glycoprotein. 10 μg of SKOV/VLB cell membranes was incubated in the presence of 0.2 μg (lanes 2 and 3), 3 μg (lane 4), and 6 μg (lane 5) of trypsin at 37 °C. The reaction duration was 15 min (lane 2), 30 min (lane 3), and 2 h (lanes 4 and 5), respectively. Lane 1 is a control of 3 μg of undigested SKOV/VLB cell membranes. Panels A−C are the same blot probed with different antibodies. A = MD-7, B = C219, and C = C494. (D and E) Panels D and E are the same blot as in panels A−C, but only the corresponding lanes 3−5 were shown. D = MD-1 and E = pAb 5. Separate experiments have also been performed with MD-1 and pAb 5, and the results are consistent with the data shown here. However, to be consistent with the panels A, B, and C, only the stripped blot was shown. (F) 10 μg of SKOV/VLB cell membranes was incubated in the presence of 3 μg of trypsin at 37 °C for 2 h (same as lane 4, panel A). The blot was probed with MM4.17. (G) 10 μg of SKOV/VLB cell membranes was incubated in the presence of 3 μg of trypsin at 37 °C for 2 h (same as in lane 4, panel A) in the absence (lane 1) or presence (lane 2) of 1% Triton X-100. The blot was probed by MD-7.

In addition to peptide C, the mAb C494 also reacted with peptide X (lanes 4 and 5, Figure 5C) which was not detected by the mAb C219 (lanes 4 and 5, Figure 5B). This peptide is likely a further degradation product from peptide C. Thus, after Pgp was cleaved into two halves, the C-terminal half molecule was further digested and the ATP-binding domain containing the mAb C219 epitope was removed, resulting in peptide X (see Figure 1 for cleavage site 2). However, the C494 epitope is still attached to the truncated C-terminal half molecule (peptide X). Both the mAb C219 and C494 did not react with peptides Y and Z, suggesting that these two peptides are further degradation products and have lost epitopes for both C219 and C494.

To determine whether peptide Z contains the linker region and loop 10, we probed the same stripped blot again with a mAb MD-1 (Shapiro et al., 1996) and a site-specific pAb 5 (Greenberger et al., 1991). As shown in Figure 1, the mAb MD-1 is specific to the linker region whereas the epitope for the pAb 5 is in loop 10. Both antibodies are specific to the C-terminal half molecule as shown by their reactivity with peptide C but not peptide N (lanes 1 and 2 in Figure 5D,E). Both antibodies also reacted with peptide X (lanes 2 and 3 in Figure 5D,E), suggesting that peptide X still contains the epitope for both antibodies. The mAb MD-1 detected, in addition, peptide Y (lane 3, Figure 5D) which, however, was not detected by the pAb 5 (lane 3, Figure 5E). Therefore, peptide Y lost the epitope for the pAb 5 but still retains the epitope for the mAb MD-1. The mAb MD-1, however, did not detect peptide Z, albeit the amount of peptide Z is higher than peptide Y (compare lane 5 in Figure 5A with lane 3 in Figure 5D). Peptides Y and Z are still on the membrane after stripping as determined using MD-7 (data not shown). These results suggest that peptide Z is a final trypsin-resistant fragment which only retains the epitope for the mAb MD-7 and does not contain the epitopes for the mAbs C219, C494, and MD-1 nor the site-specific pAb 5 (see model II in Figure 1).

To prove that peptide Z also contains loop 7 (linking TM7 and TM8) in addition to loop 8 (linking TM8 and TM9), we probed the digested products with another mAb MM4.17 of which the epitope is in loop 7 (Cianfriglia et al., 1994). As expected, the mAb MM4.17 reacted with all the peptides C, X, Y, and Z (Figure 5F). To confirm that the trypsin resistance of peptide Z was due to membrane protection, we performed a digestion in the presence of Triton X-100 to permeabilize the membrane. As shown in Figure 5G, the trypsin-resistant peptide Z was produced in the absence of Triton X-100 (lane 1, Figure 5G) but was completely digested in the presence of Triton X-100 (lane 2, Figure 5G). The above results showed that the domain containing loop 7 and loop 8 (with mAb MM4.17 and MD-7 epitopes) in inside-out vesicles is resistant to trypsin digestion whereas loop 10 (linking TM10 and TM11 with pAb 5 epitope) and the C-terminal ATP-binding domain (containing mAb C219 and C494 epitopes) are sensitive to trypsin digestion. Thus, the segment containing both loop 7 and loop 8 is likely located in the lumen of the isolated inside-out membrane vesicles (extracellular location), consistent with the model II structure in Figure 1.

*The Trypsin-Resistant Fragment Z Is Also Observed from a Cell Transfected with Human MDR1 cDNA.* To determine whether the trypsin-resistant fragment Z was due to the overexpression of Pgp in the multidrug-resistant SKOV/VLB cells, we took use of cells transfected with the human *MDR1* Pgp cDNA (BC19/3 cells). The Pgp level expressed in BC19/3 cells is less than 10% of Pgp expressed in the SKOV/VLB cells (unpublished observation). Using the same procedure, the vesicles isolated from BC19/3 cells are also all inside out as determined using acetylcholinesterase (data not shown). Trypsin digestion of the inside-out membrane vesicles from BC19/3 cells was performed. The digested fragments were subjected to a Western blot and probed with the mAb MD-7. As shown in Figure 6A, peptides C, X, Y, and Z were all detected. Therefore, generation of the trypsin-resistant fragment Z of Pgp in MDR cells is not related to the high expression levels of Pgp. Peptides C, X, Y, and Z were not detected when membranes from sensitive parental cell lines were digested by trypsin (data not shown). This result rules out the possibility that these peptides were generated from digestion of non-Pgp proteins.

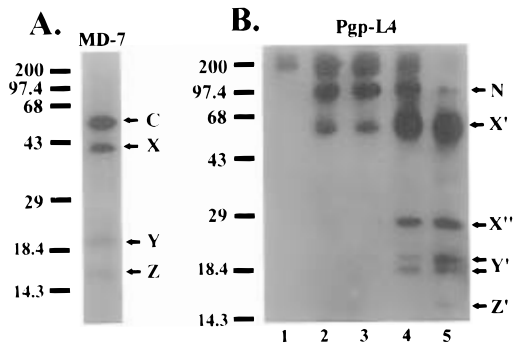


FIGURE 6: (A) Trypsin digestion of BC19/3 cell membranes. 20 $\mu$g of BC19/3 cell membranes was digested with 3 $\mu$g of trypsin at 37 °C for 2 h (same condition as in lane 4, Figure 5A). The blot was probed with the mAb MD-7. (B) Membrane protection of loop 4. The same blot from Figure 5A−C (membranes from the SKOV/VLB cells) was stripped and probed with the pAb αPgp-L4. The minimum peptide fragment Z′ is the protected loop 4 of Pgp.

*Loop 4 of Human Pgp in Inside-Out Membrane Vesicles Is Protected from Trypsin Digestion*. To determine whether the loop linking the putative TM4 and TM5 (loop 4) is also resistant to trypsin digestion in inside-out vesicles of MDR cells (SKOV/VLB), we again stripped the blot shown in Figure 5A and probed it with the pAb αPgp-L4. This antibody specifically detected peptide N (lanes 2−5, Figure 6B; see also Figure 2). In addition, further digested products X′, X″, Y′ (a doublet), and Z′ were also detected (lanes 4 and 5, Figure 6B). Peptide Z′, with an apparent molecular mass of 14.5 kDa, is the smallest trypsin-resistant fragment from the N-terminal half molecule. It presumably represents the membrane-protected fragment containing loop 4 with the epitope for the pAb αPgp-L4 whereas peptides X′, X″, and Y′ are incompletely digested products of peptide Z′. In the presence of Triton X-100, these peptides were also completely digested (data not shown). Therefore, by analogy to the study of loop 8 in the C-terminal half, it is likely that loop 4 of Pgp is also located in the lumen of the inside-out membrane vesicles (extracellular location) as shown in the model II structure in Figure 1.

## DISCUSSION

In this study, two site-specific polyclonal antibodies were produced and were used in combination with a panel of other site-specific pAbs and mAbs to show that Pgp molecules in MDR cells have the unconventional topology. Using immunocytochemistry and proteolysis/membrane protection assay, we were able to show that both loops 4 and 8 of Pgp in MDR cells can be detected extracellularly. Our results are consistent with the expression of an unconventional topology of Pgp (see Figure 1). In this study, the Pgp sequence was not altered by cDNA manipulation. We, therefore, believe that the naturally expressed Pgp has an unconventional topology. Loops 3 and 9 of Pgp are also on different sides of the membrane in the model I and model II topology of Pgp, respectively (see Figure 1). However, antibodies against these two loops were not produced to analyze their membrane sidedness due to their short length (2−6 amino acids).

We also showed that Pgp has specific trypsin-sensitive sites. That the Pgp molecule was first cleaved into two halves suggests that a domain prior to amino acid residues 669−690 (MD-1 epitope in human Pgp) linking the N- and C-terminal half Pgp is exposed and its access to trypsin is not hindered by the two bulky cytoplasmic ATP-binding domains (Figure 1). However, other trypsin-sensitive sites in the cytoplasmic loops (e.g., loop 10) are presumably buried and accessible to trypsin only when the ATP-binding domains are removed by digestion. As shown in Figure 1, other detectable trypsin cleavage sites in the C-terminal half molecule are at the ATP-binding domain and loop 10. Further work is required to identify each trypsin cleavage site. Although it is possible that loop 8 linking TM8 and TM9 is intrinsically resistant to proteolysis, we think this possibility is highly unlikely. First, loop 8 of human Pgp contains 10 Arg or Lys residues in the loop of 55 amino acids. It is unlikely that all the Arg and Lys residues are buried by the folding of this relatively small loop. Second, other predicted cytoplasmic domains including loop 10 containing the pAb 5 epitope and the large cytoplasmic ATP-binding domain are both completely digested by trypsin. Third, loop 8 was colocalized with loop 7 in the same trypsin-resistant peptide fragment and was detectable on the extracellular surface.

Different unconventional topologies have been described by Zhang and Ling (1991), Skach et al. (1993), and Bibi and Béjà (1994), respectively. However, the common feature between all the unconventional topologies is that the loop linking TM8 and TM9 is extracellular, different from the predicted conventional topology. In this study, we have shown that loop 8 can be detected on the outside of cells, consistent with the previous studies using heterologous expression systems. The estimated size of the trypsin-resistant fragments is consistent with one of the unconventional model (Figure 1) proposed previously (Zhang et al., 1993). However, from this study, we cannot rule out the possibility that the predicted topology (model I, Figure 1) is also expressed in the MDR cells. In fact, more staining using pAb αPgp-L8 was observed when cells were permeabilized (Figure 4), suggesting that loop 8 is also located intracellularly. It is worth noting that expression of more than one topology has been observed with prion protein (Lopez et al., 1990), ductin (Alves et al., 1993), bile acid transporter (Dunlop et al., 1995), and hepatitis B virus envelope proteins (Prange & Streeck, 1995).

The estimated molecular masses of the protease-resistant fragments Z (17 kDa) and Z′ (14.5 kDa) are 2 kDa smaller than the ones (19 and 16.5 kDa, respectively) predicted on the basis of amino acid sequence and the unconventional topology in inside-out vesicles shown in Figure 1. This is probably due to the high hydrophobicity of these peptides each containing three to four putative transmembrane segments. High hydrophobicity will cause more binding of SDS and therefore results in a faster mobility on SDS−PAGE. However, due to the anonymous mobility of peptide fragments on SDS−PAGE, the unconventional topologies of Pgp as proposed by Skach et al. (1993) and by Béjà and Bibi (1995) cannot be ruled out.

Recently, Kast et al. (1995) examined the topology of mouse *mdr3* Pgp using epitope insertion and confirmed the extracellular location of putative loops 1 and 5 and the intracellular location of putative loops 2 and 6. This is consistent with both model I and model II structures shown in Figure 1. Unfortunately, the membrane sidedness of the loop linking putative TM3 and TM4 and the loop linking putative TM4 and TM5 was not examined by these authors (see discussion below). The topology of human *MDR1* Pgp has also been examined by expression of cysteine-less mutant Pgp in mammalian cells, and only the predicted topology (model I, Figure 1) was detected (Loo & Clarke, 1995). The discrepancy between these studies is currently not known. However, it may be due to the different expression systems used. It has been observed that cytoplasmic proteins expressed in different systems are involved in the regulation of topology formation of hamster Pgp (Zhang & Ling, 1995). Expression of the homologous cytoplasmic proteins in different mammalian cells may make a difference in the topological formation of Pgp. It is also possible that both the conventional and unconventional topologies of Pgp exist and interchange during drug transport (see discussion below).

It is interesting to note that the hydrophobic segments TM3 and TM5 in the N-terminal half and TM8 and TM10 in the C-terminal half of the unconventional topology of Pgp are not in the membrane. These hydrophobic segments may participate in binding and transporting lipophilic chemotherapeutic drugs. Recently, it has been shown that mutation of the proline residues in the putative TM10 of human *MDR1* Pgp drastically altered the resistance profile of the cells carrying the mutant Pgp (Loo & Clarke, 1993). This observation suggests that the putative TM10 may be involved in recognizing, binding, or transporting the cytotoxic drugs. Insertion of an epitope into the loop linking putative TM3 and TM4 and the loop linking putative TM4 and TM5 disrupted the function of mouse *mdr3* Pgp (Kast et al., 1995), suggesting that these regions are important for the drug transport function.

It is therefore tempting to propose that the unconventional topology of Pgp represents a different functional state of the molecule. The cytoplasmically located hydrophobic segments TM3 and TM10 and their flanking sequences may be involved in binding drugs in cytoplasm. By conformational change, the TM3 and TM10 may help translocate the drug substrate from the cytoplasm to the outside of cells where the extracellularly located hydrophobic segments TM5 and TM8 and their flanking sequences are involved in releasing drugs. It is also possible that this drug transport process involves the conversion of the two different topologies of Pgp supported by the energy obtained from ATP hydrolysis. Recently, the gating of colicin Ia, a voltage-sensitive channel, has been shown to involve a massive change in membrane topology between the opening and closed states (Slatin et al., 1995). At least 31 amino acids of the colicin Ia located in the *cis* side of the membrane appear to be translocated to the *trans* side of the membrane when the channel changes from the closed state to the open state. Further study of the relationship between topology and function of Pgp will elucidate the underlying drug transport mechanism.

## ACKNOWLEDGMENT

The authors thank Dr. Victor Ling for providing Aux B1, $CH^RB30$, and SKOV/VLB cell lines, mAbs C219 and C494, the C219 epitope peptide analog, and hamster *pgp1* cDNA; Dr. Susan Horwitz for pAb 5; Dr. Maurizio Cianfriglia for mAb MM4.17; and Dr. Guillermo Altenberg for BC19/3 cells

and for the assistance in use of the confocal fluorescence microscope. We also thank Drs. Guillermo Altenberg, Karl Karnaky, Jr., and Luis Reuss for their critical comments on the manuscript.

## REFERENCES

Alves, C., von Dippe, P., Amoui, M., & Levy, D. (1993) *J. Biol. Chem. 268*, 20148−20155.
Béjà, O., & Bibi, E. (1995) *J. Biol. Chem. 270*, 12351−12354.
Bender, W. W., Garan, H., Berg, H. C. (1971) *J. Mol. Biol. 58*, 783−797.
Bibi, E., & Béjà, O. (1994) *J. Biol. Chem. 269*, 19910−19915.
Borst, P., Schinkel, A. H., Smit, J. J., Wagenaar, E., van Deemter, L., Smith, A. J., Eijdems, E. W., Baas, F., & Zaman, G. J. (1993) *Pharmacol. Ther. 60*, 289−299.
Bradley, G., Naik, M., & Ling, V. (1989) *Cancer Res. 49*, 2790−2796.
Chifflet, S., Torriglia, A., Chiesa, R., & Tolosa, S. (1988) *Anal. Biochem. 168*, 1−4.
Childs, S., & Ling, V. (1994) in *Important Advances in Oncology* (DeVita, V. T., Hellman, S., & Rosenberg, S. A., Eds.) pp 21−36, Lippincott Co., Philadelphia, PA.
Cianfriglia, M., Willingham, M. C., Tombesi, M., Scagliotti, G. V., Frasca, G., & Cherst, A. (1994) *Int. J. Cancer 56*, 153−160.
Doige, C. A., & Ames, G. F.-L. (1993) *Annu. Rev. Microbiol. 47*, 291−319.
Doige, C. A., Yu, X., & Sharom, F. J. (1992) *Biochim. Biophys. Acta 1109*, 149−160.
Dunlop, J., Jones, P., & Finbow, M. E. (1995) *EMBO J. 14*, 3609−3616.
Endicott, J. A., Sarangi, F., & Ling, V. (1991) *DNA Sequence 2*, 89−101.
Georges, E., Bradley, G., Gariepy, J., & Ling, V. (1990) *Proc. Natl. Acad. Sci. U.S.A. 87*, 152−156.
Georges, E., Zhang, J. T., & Ling, V. (1991) *J. Cell. Physiol. 148*, 479−484.
Georges, E., Tsuruo, T., & Ling, V. (1993) *J. Biol. Chem. 268*, 1792−1998.
Gottesman, M. M., & Pastan, I. (1993) *Annu. Rev. Biochem. 62*, 385−427.
Greenberger, L. M., Lisanti, C. J., Silva, J. T., & Horwitz, S. B. (1991) *J. Biol. Chem. 266*, 20744−20751.
Harlow, E., & Lane, D. (1988) *Antibodies, a laboratory manual*, Cold Spring Harbor Laboratory, Cold Spring Harbor, NY.
Higgins, C. (1992) *Annu. Rev. Cell Biol. 8*, 67−113.
Kartner, N., Evernden-Porelle, D., Bradley, G., & Ling, V. (1985) *Nature 316*, 820−823.
Kast, C., Canfield, V., Levenson, R., & Gros, P. (1995) *Biochemistry 34*, 4402−4411.
Loo, T. W., & Clarke, D. M. (1993) *J. Biol. Chem. 268*, 3143−3149.
Loo, T. W., & Clarke, D. M. (1995) *J. Biol. Chem. 270*, 843−848.
Lopez, C. D., Yost, C. S., Prusinger, S. B., Myers, R. M., & Lingappa, V. R. (1990) *Science 248*, 226−229.
Prange, R., & Streeck, R. E. (1995) *EMBO J. 14*, 247−256.
Riordan, J. R., & Ling, V. (1979) *J. Biol. Chem. 254*, 12701−12705.
Shapiro, A. B., Duthie, M., Childs, S., Okubo, T., & Ling, V. (1996) *Int. J. Cancer* (in press).
Skach, W. R., & Lingappa, V. R. (1993) *J. Biol. Chem. 268*, 23552−23561.
Skach, W. R., Calayag, M. C., & Lingappa, V. R. (1993) *J. Biol. Chem. 268*, 6903−6908.
Slatin, S. L., Qiu, X.-Q., Jakes, K. S., & Finkelstein, A. (1995) *Nature 371*, 158−161.
Steck, T. L., & Kant, J. A. (1974) *Methods Enzymol. 31*, 172−180.
Zhang, J. T., & Ling, V. (1991) *J. Biol. Chem. 266*, 18224−18232.
Zhang, J. T., & Ling, V. (1995) *Biochemistry 34*, 9159−9165.
Zhang, J. T., Duthie, M., & Ling, V. (1993) *J. Biol. Chem. 268*, 15101−15110.
Zhang, J. T., Lee, C.-H., Duthie, M., & Ling, V. (1995) *J. Biol. Chem. 270*, 1742−1746.
Zhang, M., & Zhang, J. T. (1995) *Proc. Am. Assoc. Cancer Res. 36*, 337a.

BI960400S